Role of Surface Electronic Structure in Thin Film Molecular Ordering

G. E. Thayer,[1] J. T. Sadowski,[2] F. Meyer zu Heringdorf,[3] T. Sakurai,[2] and R. M. Tromp[4]

[1]*Sandia National Laboratories, P. O. Box 5800, Albuquerque, New Mexico 87185-1427, USA*

[2]*Institute for Materials Research, Tohoku University, Sendai 980-8577, Japan*

[3]*Institute of Laser and Plasma Physics, University of Duisburg-Essen, Universitätsstrasse 5, D-45117 Essen, Germany*

[4]*IBM Research Division, T. J. Watson Research Center, 1101 Kitchawan Road, P.O. Box 218, Yorktown Heights, New York 10598, USA*

(Received 19 July 2005; published 16 December 2005)

We show that the orientation of pentacene molecules is controlled by the electronic structure of the surface on which they are deposited. We suggest that the near-Fermi level density of states above the surface controls the interaction of the substrate with the pentacene π orbitals. A reduction of this density as compared to noble metals, realized in semimetallic Bi(001) and Si(111)(5×2)Au surfaces, results in pentacene standing up. Interestingly, pentacene grown on Bi(001) is highly ordered, yielding the first vertically oriented epitaxial pentacene thin films observed to date.

DOI: 10.1103/PhysRevLett.95.256106 PACS numbers: 68.37.Nq, 61.66.Hq, 68.55.Ac

While inorganic materials such as silicon and gallium arsenide have long been foundations of the microelectronics industry, there is now a growing interest in the use of organic semiconductors. Pentacene (Pn), in particular, has attracted attention since it has shown promise in organic thin-film transistors (OTFT's), with field-effect mobilities surpassing that of amorphous silicon [1]. However, organic electronics faces a number of challenges that require fundamental understanding to make significant progress. In an OTFT the semiconductor is in intimate contact with several disparate insulating and metallic materials. Structural integrity and uniformity of the semiconductor across these different interfaces is highly desirable for optimum device performance, but difficult to achieve. Similarly, in molecular electronics it is hoped that small numbers or even single molecules can be utilized to realize devices with novel properties [2]. In all these cases, the structural, chemical, and electrical properties of the interfaces to a large extent determine charge carrier injection and device stability and are thus exceedingly important for technological applications.

Also important for thin-film electronic devices is the degree of crystallinity and the lateral extent of the crystalline domain. Domain boundaries, crystal defects, and impurities are often detrimental for charge transport. Epitaxial growth has long been used in inorganic semiconductors to create films and superlattices with a high degree of order and low defect density. Here we show that Pn can be grown epitaxially on lattice-matched semimetallic substrates, promising new avenues for the development of improved organic electronic materials and devices.

The growth of Pn can act as a model system to develop our understanding of key aspects of the interaction of simple organic molecules with a variety of different surfaces as may be encountered in thin-film organic or molecular devices. Previous studies of Pn growth on noble metals such as Au [3], Ag [4], and Cu [5] have shown that the molecule lies down on the surface, whereas on insulating surfaces such as SiO_2 [6], Al_2O_3 [7], or organically terminated Si [8] the molecules stand up. Here we show that the orientation of the molecule is controlled by the substrate electronic structure. Pn, while lying down on metallic surfaces, stands up on weakly metallic or semimetallic substrates such as Bi(001) [9] or the Si(111)-(5×2)Au surface [10]. We suggest that the interaction strength of the Pn π system with the substrate is controlled by the local density of states (LDOS) at or near the Fermi level at the substrate surface. At low electron density van der Waals interactions dominate, and the π-π interactions between Pn molecules are stronger than the interactions with the substrate. But as the surface LDOS is increased molecule-substrate interactions become stronger, and the molecule switches orientation from standing up to lying down. On the semimetallic Si(111)-(5×2)Au surface the molecule-surface interaction is weak and the molecule stands up. However, addition of less than 0.5 monolayers of Au to the Si(111)-(5×2)Au structure results in the metallic Si(111)-$(\sqrt{3} \times \sqrt{3})$Au surface on which we find Pn to lie down flat. This dramatically illustrates how small changes in surface preparation can lead to large changes in surface-molecule interaction.

The experiments were performed using *in situ* low energy electron microscopy (LEEM) and photo electron emission microscopy (PEEM) [11], as well as microbeam low energy electron diffraction (LEED), and scanning tunneling microscopy (STM). PEEM images were obtained using a 100 W high pressure Hg discharge lamp as a UV source. Bi(001) was prepared by growing $\sim$15 ML of Bi on clean Si(111)(7×7) at room temperature [9]. Si(111)(5×2)Au was prepared by exposing the clean Si(111)(7×7) surface at $\sim$600 °C to an Au flux from a small evaporator until the LEED pattern had fully converted to $(5 \times 2$. Deposition of additional Au results in the formation of Si(111)$(\sqrt{3} \times \sqrt{3})$Au, as monitored by LEEM and LEED. Pn films were grown at room temperature from a water-cooled quartz Knudsen cell heated to

~250 °C [8]. *In situ* STM experiments were performed at Tohoku University. Sample preparation conditions closely matched those used in the LEEM/PEEM experiments at IBM.

Figure 1(a) and 1(b) shows PEEM/LEEM images and corresponding LEED patterns for Pn grown on Si(111)(5 × 2)Au [Fig. 1(a)], and on Si(111)($\sqrt{3} \times \sqrt{3}$)Au [Fig. 1(b)]. On the (5 × 2)Au surface, Pn with a thickness of a single molecular layer shows a LEED pattern typical of Pn standing up, with in-plane lattice parameters $a = 6.1 \pm 0.2$ Å, $b = 7.6 \pm 0.2$ Å, $\gamma = 90° \pm 1°$, close to bulk Pn [for the low density polymorph of Pn: $a =$ 6.06 Å, $b = 7.90$ Å, $\gamma = 85.8°$ [12]]. While the LEED pattern shows that the Pn is not epitaxially aligned with the Si substrate, the sharpness of the Pn spots demonstrate that the film is highly ordered.

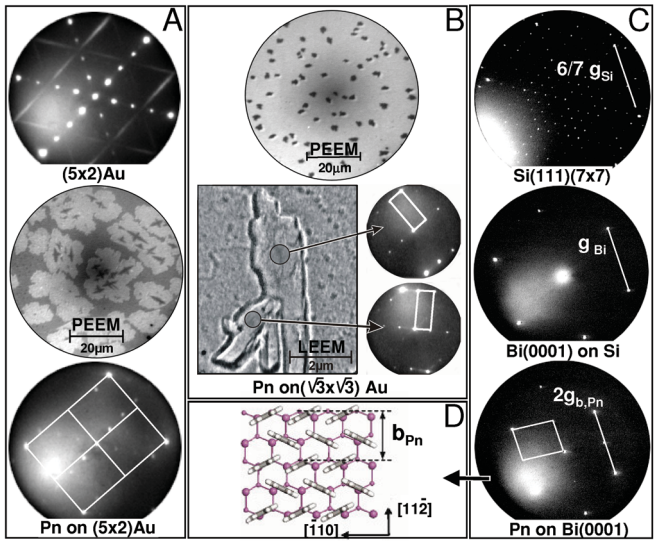

FIG. 1 (color). (a) Top: LEED pattern of the semimetallic Si(111)(5 × 2)Au surface before Pn deposition. Middle: PEEM image of a submonolayer Pn film grown on top of this surface. The PEEM image shows monolayer high Pn island with a lateral extent of ~20 μm (light gray on a darker gray background). On top of these islands "daggerlike" second layer Pn islands can be seen to have nucleated before the first layer fully closes; bottom: microbeam LEED pattern obtained on this Pn film. White outlines show 4 reciprocal Pn unit cells. There is no exact azimuthal alignment between the Pn and underlying (5 × 2)Au lattices. (b) Top: PEEM image of Pn grown on the metallic Si(111)($\sqrt{3} \times \sqrt{3}$)Au surface. Rather than the 2D islands seen in (a), this image shows agglomeration on Pn in 3D islands (dark spots). Bottom: LEEM image of a 3D Pn island, and selective area microbeam LEED patterns obtained on this island. Pn LEED unit cells are outlined in white, and show that the Pn molecules are parallel to the surface. (c) LEED patterns obtained on the clean Si(111)(7 × 7) surface (top), the epitaxial Bi(001) film (middle), and a monolayer of Pn grown on the Bi(001) surface (bottom). The identical white line segments shown in each pattern show that $6/7\mathbf{g}_{\mathrm{Si}} = \mathbf{g}_{\mathrm{Bi}} = 2\mathbf{g}_{\mathrm{b,Pn}}$, highlighting the close epitaxial relationships between these three lattices. The Pn LEED unit cell is also shown in the bottom panel. Note: the LEED patterns in panels (a), (b), and (c) are not at the same magnification. (d) Schematic model of the Bi(001)/Pn interface as derived from the LEED patterns shown in panel (c).

On the ($\sqrt{3} \times \sqrt{3}$)Au surface [Fig. 1(b)], Pn agglomerates in a number of 3D islands (black dots in the PEEM image), and the microbeam LEED patterns of one of these islands show that the molecules are oriented parallel to the substrate surface. Further illustrating the 3D growth mode on the ($\sqrt{3} \times \sqrt{3}$)Au surface, Fig. 2(a) shows an AFM image of two Pn islands grown in the LEEM. The atomic steps of the ($\sqrt{3} \times \sqrt{3}$)Au surface between the large 3D Pn islands can be clearly distinguished. The linescan in Fig. 2(b) shows that the Pn islands have a height of ~55 nm, or about 35 molecular layers. The LEED unit cell [highlighted white in the LEED patterns in Fig. 1(b)] shows in-plane lattice vectors of 15.7 ± 0.8 Å and 6.51 ± 0.3 Å, close to the bulk c and a lattice constants. This change of molecular orientation is correlated with the change in surface electronic structure from semimetallic (5 × 2)Au to metallic ($\sqrt{3} \times \sqrt{3}$)Au. Specifically, for the molecular adsorption discussed here, it is the *surface* LDOS that matters, not the substrate DOS. Going from Si(111)(5 × 2)Au to Si(111)-($\sqrt{3} \times \sqrt{3}$)Au, the bulk DOS obviously does not change. Instead, it is the rather subtle change in the surface LDOS, specifically the change from semimetallic to metallic, i.e., the change in surface valence charge density at or near the Fermi level, that leads to the observed change in molecular orientation.

Figure 1(c) shows the results for Pn grown on Bi. As for the (5 × 2)Au surface, diffraction shows that the molecule stands up, with in-plane lattice parameters close to bulk Pn. However, we also observe another striking feature. The LEED patterns in Fig. 1(c), for clean (7 × 7), Bi(001), and Pn on Bi(001) each have an identical length reciprocal

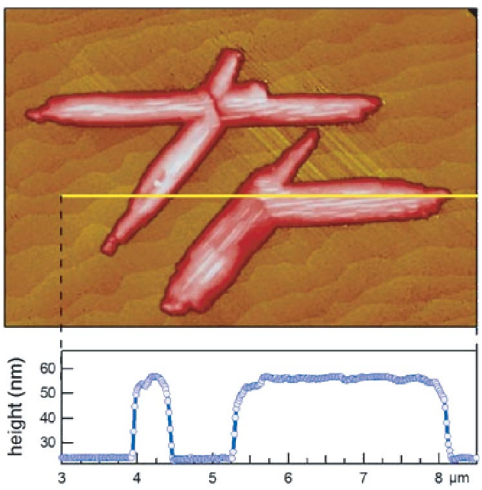

FIG. 2 (color). (a) Tapping-mode AFM image of 3D Pn island grown on Si(111)($\sqrt{3} \times \sqrt{3}$)Au. (b) Linescan demonstrating the ~55 nm height of the Pn islands.

lattice vector inserted for comparison (white line). The fact the $\mathbf{g}_{Bi} = 6/7\ \mathbf{g}_{Si}$ shows that Bi grows on the (7×7) surface, with 6 Bi lattice spacings providing an epitaxial match with 7 Si lattice spacings. But additionally, this same lattice vector also measures the distance of 2 Pn reciprocal lattice vectors along the Pn reciprocal b direction, i.e., $\mathbf{g}_{Bi} = 2\mathbf{g}_{b,Pn}$. That is, the Pn lattice closely matches the Bi lattice, such that the 2nd order Pn diffraction spots coincide with the 1st order Bi spots. The Pn lattice spacings derived from this LEED pattern are: $a = 6.1 \pm 0.2$ Å, $b = 7.89$ Å (no error bar given as the Pn diffraction spot overlaps with the Bi diffraction spot), and $\gamma = 86 \pm 0.5$ degrees, close to the bulk spacings of Pn [12]. Figure 1(d) shows a schematic view of the alignment of the Bi and Pn lattices in real space, in which Pn molecules align incommensurately with the Bi lattice along the $[\bar{1}10]$ direction, and commensurately along the $[11\bar{2}]$ direction.

Crystallographic alignment of Pn molecules has been observed previously on metallic surfaces on which the molecules lie down flat [5], but not on surfaces on which the molecules stand up, and we believe this to be the first observation of an epitaxial Pn thin film in this crystal orientation. This is an important observation from the point of view of Pn TFT applications, for which the molecules must stand up for the high mobility direction to align with the current path from source to drain.

In situ STM images of Pn grown on Bi(001) are shown in Fig. 3. In the linescan of a second layer Pn island on Bi [Fig. 3(a)] we can distinguish the ~1.5 nm step height associated with Pn standing up, as well as the ~0.4 nm steps associated with the underlying Bi. The sharpness of the LEED patterns in Fig. 1(c) suggests a very high degree of molecular order, as is born out by the STM experiments [Fig. 3(c)], in which the Pn molecular lattice is easily resolved and found to be highly ordered.

It is interesting that the interaction between Pn and the substrate is sufficiently weak to allow the molecules to stand up, yet sufficiently strong to align the Pn lattice with substrate. This was explored in more detail with *in situ* STM. Figures 3(d) and 3(e) show another bilayer Pn island crossing several atomic terraces of the underlying Bi film both before (d) and after (e) applying a 3.5 V pulse to the STM tip, to locally desorb Pn. After the pulse, a small hole has opened in the Pn film [Fig. 3(e)]. A linescan through the hole reveals a step height of ~3 nm, the thickness of two Pn layers. An atomic resolution image of the bottom of the hole reveals the atoms in the Bi surface [Fig. 3(f)]. This image is essentially identical to images obtained on clean Bi substrates, indicating that the interaction between Bi and Pn is indeed quite weak, and does not involve the formation of chemical bonds. The applied voltage pulse removes the Pn, leaving an atomically clean and ordered Bi surface behind. Figures 3(c) and 3(f) are shown on the same scale, graphically demonstrating the close match between the Bi and Pn lattices [Fig. 1(d)].

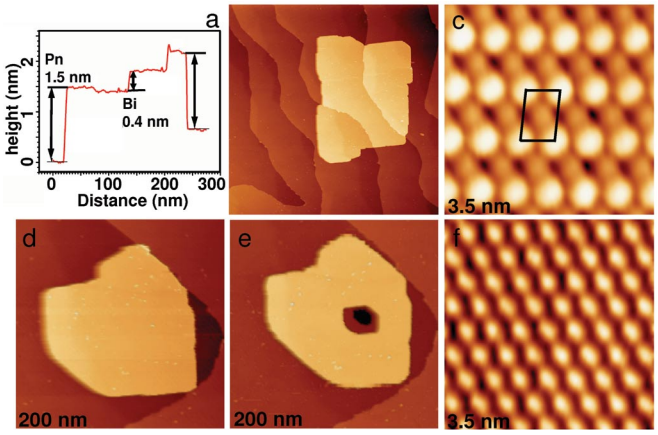

FIG. 3 (color). (a) Vertical height plot along the black line shown in (b). (b) STM image of a monolayer of Pn covering the Bi(001) surface, with a second layer of Pn overgrowing several underlying Bi terraces in the center of the image. (c) High resolution STM image (sample bias +1.6 V) showing individual Pn molecules in the first layer. A single Pn unit cell containing 2 Pn molecules (corners and center) is outlined in black. (d) Second layer Pn film (center) on top of a continuous monolayer of Pn on Bi(001). (e) Same layer after application of a 3.6 V pulse to the STM tip, opening a 2 layer deep hole in the Pn island. The bare Bi surface is exposed at the bottom of the hole. (f) Atomic resolution image of underlying Bi lattice. Note the close correspondence between the Pn and Bi lattices by comparing (c) and (f).

We have shown that the molecular orientation in thin Pn films grown on a variety of surfaces is directly related to the electronic structure of the substrates. On metallic surfaces, the molecules interact strongly with the surface valence charge density near the Fermi level, leading to planar adsorption geometry. As this valence charge density is reduced, the molecule-molecule interaction becomes stronger than the molecule-substrate interaction. This results in the Pn molecules standing up on the surface. However, the Pn-surface interaction is still sufficiently strong to give rise to alignment of the Pn lattice with the substrate crystal directions. On amorphous insulating surfaces, the interaction of Pn with the substrate is van-der-Waals-like, and the molecules stand up. In that case, different grains have no common in-plane crystal orientation, and thicker Pn films contain numerous large-angle grain boundaries. Growth on semimetallic surfaces provides an avenue to balance the intermolecular and molecule-substrate interactions, where the former are sufficiently strong to allow the molecules to stand up, and the latter sufficiently significant to lock the Pn lattice to the underlying substrate. Careful control of the substrate electronic structure provides a new avenue to controlling the molecular orientation of thin organic films.

F. M. z. H. acknowledges financial support from the Humboldt Foundation under the Feodor-Lynen programme.

[1] Y.-Y. Lin, D. J. Gundlach, S. F. Nelson, and T. N. Jackson, IEEE Trans. Electron Devices **44**, 1325 (1997); C. Dimitrakopoulos, A. Brown, and A. Pomp, Science **283**, 822 (1999); H. Klauk and T. Jackson, Solid State Technol. **43**, 63 (2000);

[2] J. M. Tour, *Molecular Electronics; Commercial Insights, Chemistry, Devices, Architecture and Programming* (World Scientific, Singapore, 2003).

[3] J. H. Kang and X.-Y. Zhu, Appl. Phys. Lett. **82**, 3248 (2003); P. G. Schroeder, C. B. France, J. B. Park, and B. A. Parkinson, J. Appl. Phys. **91**, 3010 (2002); G. Beemink, T. Strunskus, G. Witte, and Ch. Wöll, Appl. Phys. Lett. **85**, 398 (2004).

[4] Y. L Wang, W. Ji, D. X. Shi, S. X. Du, C. Seidel, Y. G. Ma, H.-J. Gao, L. F. Chi, H. Fuchs, Phys. Rev. B **69**, 075408 (2004); L. Casalis, M. F. Danisman, B. Nickel, G. Bracco, T. Toccoli, S. Iannotta, and G. Scoles, Phys. Rev. Lett. **90**, 206101 (2003).

[5] L. Lukas, G. Witte, and Ch. Wöll, Phys. Rev. Lett. **88**, 028301 (2002); S. Lukas, S. Sönchen, G. Witte, and Ch. Wöll, Chem. Phys. Chem. **5**, 266 (2004).

[6] R. Ruiz, B. Nickel, N. Koch, L. C. Feldman, R. F. Haglund, A. Kahn, and G. Scoles, Phys. Rev. B **67**, 125406 (2003); R. Ruiz, B. Nickel, N. Koch, L. C. Feldman, R. F. Haglund, A. Kahn, F. Family, and G. Scoles, Phys. Rev. Lett. **91**, 136102 (2003); S. Pratontep, M. Brinkman, F. Nüesch, and L. Zuppiroli, Phys. Rev. B **69**, 165201 (2004); S. E. Fritz, S. M. Martin, C. D. Frisbie, M. D. Ward, and M. F. Toney, J. Am. Chem. Soc. **126**, 4084 (2004).

[7] W. Kalb, P. Lang, M. Mottaghi, H. Aubin, G. Horowitz, and M. Wuttig, Synth. Met. **146**, 279 (2004).

[8] F.-J. Meyer zu Heringdorf, M. C. Reuter, and R. M. Tromp, Nature (London) **412**, 517 (2001); F.-J. Meyer zu Heringdorf, M. C. Reuter, and R. M. Tromp, Appl. Phys. A **78**, 787 (2004); K. P. Weidkamp, C. A. Hacker, M. P. Schwartz, X. Cao, R. M. Tromp, and R. J. Hamers, J. Phys. Chem. B **107**, 11 142 (2003).

[9] T. Nagao, J. T. Sadowski, M. Saito, S. Yaginuma, Y. Fujikawa, T. Kogure, T. Ohno, Y. Hasegawa, S. Hasegawa, and T. Sakurai, Phys. Rev. Lett. **93**, 105501 (2004) and references therein. J. T. Sadowski, T. Nagao, S. Yaginuma, Y. Fujikawa, A. Al-Mahboob, K. Nakajima, T. Sakurai, G. E. Thayer, and R. M. Tromp, Appl. Phys. Lett. **86**, 073109 (2005).

[10] R. Losio, K. N. Altmann, and F. J. Himpsel, Phys. Rev. Lett. **85**, 808 (2000); K. N. Altmann, J. N. Crain, A. Kirakosian, J.-L. Lin, D. Y. Petrovykh, F. J. Himpsel, and R. Losio, Phys. Rev. B **64**, 035406 (2001) and references therein.

[11] E. Bauer, Rep. Prog. Phys. **57**, 895 (1994); R. M. Tromp, IBM J. Res. Dev. **44**, 503 (2000).

[12] R. B. Campbell, J. M. Robertson, and J. Trotter, Acta Crystallogr. **14**, 705 (1961).